Ecology, 96(2), 2015, pp. 403–416

Whole-stream ^{13}C tracer addition reveals distinct fates of newly fixed carbon

ERIN R. HOTCHKISS[1] AND ROBERT O. HALL, JR.

Program in Ecology and Department of Zoology and Physiology, University of Wyoming, Laramie, Wyoming 82071 USA

Abstract. Many estimates of freshwater carbon (C) fluxes focus on inputs, processing, and storage of terrestrial C; yet inland waters have high rates of internally fixed (autochthonous) C production. Some fraction of newly fixed C may be released as biologically available, dissolved organic C (DOC) and stimulate microbial-driven biogeochemical cycles soon after fixation, but the fate of autochthonous C is difficult to measure directly. Tracing newly fixed C can increase our understanding of fluxes and fate of autochthonous C in the context of freshwater food webs and C cycling. We traced autochthonous C fixation and fate using a dissolved inorganic C stable isotope addition ($^{13}C_{DIC}$). We added $^{13}C_{DIC}$ to North Fork French Creek, Wyoming, USA during two days in August. We monitored changes in ^{13}C pools, fluxes, and storage for 44 d after the addition. Two-compartment flux models were used to quantify net release of newly fixed $^{13}C_{DOC}$ and $^{13}C_{DIC}$ into the water column. We compared net ^{13}C fixation with tracer $^{13}C_{DIC}$ removal and gross primary production (GPP) to account for the mass of tracer fixed, released, lost to the atmosphere, and exported downstream. Much of the fixed C turned over rapidly and did not enter longer-term storage pools. Net C fixed was 70% of GPP measured with O_2. Algae likely released the remaining 30% via $^{13}C_{DOC}$ exudation and respiration of newly fixed C. Primary producers released $^{13}C_{DOC}$ at rates of up to 16% per day during the ^{13}C addition, but exudation of new labile C declined to near zero by day 6. DIC production from newly fixed C accounted for 21% of ecosystem respiration the day after the ^{13}C addition. All measured organic C (OC) pools were enriched with ^{13}C 1 d after the tracer addition. 20% of fixed ^{13}C remained in benthic OC by day 44, and average residence time of autochthonous C in benthic OC was 62 d. Newly fixed C had two distinct fates: short-term (<1 week) exudation and respiration or longer-term storage and downstream export. Autochthonous C in streams likely fuels short-term microbial production and biogeochemical cycling, in addition to providing a longer-term resource for consumers.

Key words: *^{13}C tracer; autochthonous; C cycling; DOC exudation; ecosystem metabolism; residence time; stable isotopes; streams.*

INTRODUCTION

Freshwater ecosystems play a central role in the global carbon (C) cycle. Because they are so closely connected to the surrounding landscape, inland waters support biological processes that link and integrate terrestrial, atmospheric, and ocean biogeochemical cycles (Cole et al. 2007, Aufdenkampe et al. 2011). Networks of streams, lakes, and rivers store, process, and release at least one-half of the C they receive from terrestrial ecosystems (Cole et al. 2007, Aufdenkampe et al. 2011, Raymond et al. 2013) and are net sources of carbon dioxide (CO_2) to the atmosphere, because they transport and process terrestrial CO_2 and organic C (OC) in addition to internally fixed (autochthonous) OC (Cole and Caraco 2001, Battin et al. 2008). Because terrestrial inputs to inland waters can dominate C cycling and subsidize food webs, understanding the processing and fate of terrestrial C has been a high priority in aquatic ecology (Fisher and Likens 1973, Webster 2007, Lapierre et al. 2013).

Current models of freshwater C fluxes largely focus on inputs, processing, outgassing, and storage of terrestrial C (Cole et al. 2007, Aufdenkampe et al. 2011, Regnier et al. 2013), yet many freshwater ecosystems also have high rates of internal C fixation by photosynthesis. For example, open-canopy streams and large rivers rely on autochthonous OC for a large proportion of ecosystem C cycling (Minshall et al. 1985, Webster 2007). In fact, autochthonous OC supports energy flow across multiple trophic levels in most freshwater ecosystems, even those receiving large terrestrial OC subsidies (Minshall 1978, Thorp and Delong 2002, Pace et al. 2004). C fixation and fate is not explicitly included in most freshwater C budgets because of the assumed net zero effect of fixation and respiration of autochthonous C over long time scales. However, ~0.3 Pg autochthonous C/y may be buried in or exported from inland waters (Regnier et al. 2013). The biogeochemical significance and fate of

Manuscript received 2 April 2014; revised 8 July 2014; accepted 24 July 2014. Corresponding Editor: W. V. Sobczak.

[1] Present address: Department of Ecology and Environmental Science, Umeå University, 90187, Umeå, Sweden. E-mail: ehotchkiss@gmail.com

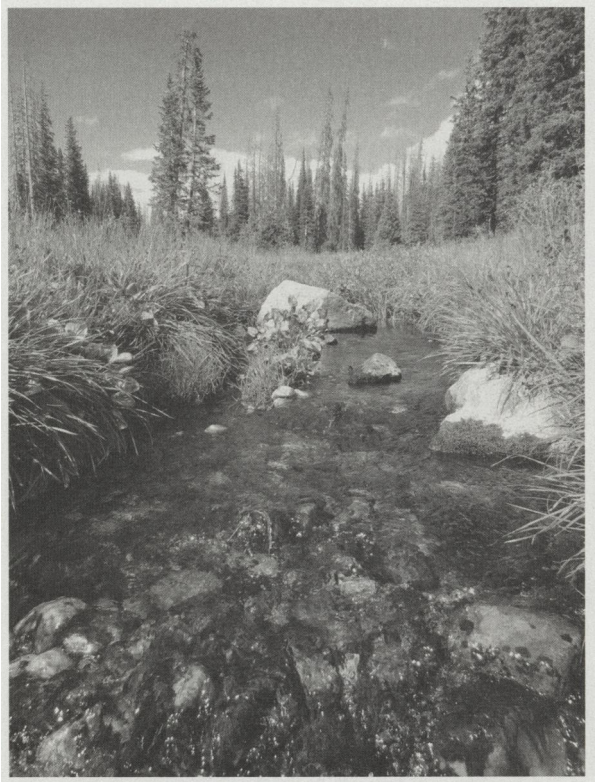

FIG. 1. Upper reach of French Creek, Medicine Bow National Forest, Wyoming, USA. Photo credit: E. R. Hotchkiss.

autochthonous C deserves further attention, not only to quantify the role of autochthonous C in larger scale budgets but also to understand the distinct fates of different C sources within freshwater food webs and C fluxes.

Despite the role of autochthonous C in supporting food webs and ecosystem C cycling, it is difficult to quantify the contribution of autochthonous C to total C fluxes. Autochthonous biomass likely turns over very quickly. Some net production is released as labile dissolved organic C (DOC), which is available to stream heterotrophic microbial assemblages (Cole et al. 1982, Kritzberg et al. 2005, Guillemette et al. 2013). Thus, while we can measure rates of gross primary and net ecosystem production in freshwater ecosystems over daily, seasonal, and multiannual timescales (Roberts et al. 2007), we cannot use ecosystem metabolism to trace the ultimate fate of autochthonous C for food web studies and C cycling budgets. ^{13}C tracers can quantify the pathways and rates of C cycling in freshwater ecosystems that may not be detected by changes in C concentrations alone (Hall 1995, Cole et al. 2002, Lyon and Ziegler 2009). The use of whole-ecosystem ^{13}C tracers originated with stream $^{13}C_{DOC}$ additions (Hall 1995, Hall and Meyer 1998), but many tracer studies have used $^{13}C_{DIC}$ (or $^{14}C_{DIC}$; dissolved inorganic C) to estimate C fixation and terrestrial C subsidies in lakes (Bower et al. 1987, Pace et al. 2004, Carpenter et al. 2005) and the fate of C in estuarine and marine assemblages (Middleburg et al. 2000, Van den Meersche et al. 2004, Oakes et al. 2012). To date, there are no analogous experimental studies of autochthonous C fate and transport in streams (but see Lyon and Ziegler [2009] and Risse-Buhl et al. [2012] for ^{13}C microcosm studies). Unlike marine and lacustrine research, ecologists are just beginning to understand how streams and rivers process and transport different C sources at large spatial scales. In addition, techniques for measuring and modeling isotope transport in streams are relatively new (Wollheim et al. 2001, Johnson et al. 2013).

We conducted a $^{13}C_{DIC}$ tracer (as $NaH^{13}CO_3$) experiment in an open-canopy mountain stream to answer the following questions about autochthonous C fixation and fate: How much recently fixed C is released as DOC and respired as DIC? How long is the residence time of autochthonous C in different pools of primary producers? How can we use ecosystem metabolism and tracer C fluxes to identify short- and long-term fates of autochthonous C? We sampled stream C pools before, during, and after the $^{13}C_{DIC}$ tracer addition. We modeled rates of autochthonous DOC and DIC production using fluxes of tracer ^{13}C into primary producer biomass, DOC, and DIC. In addition, $^{13}C_{DIC}$ uptake and fluxes were linked with rates of ecosystem metabolism to estimate whole-stream respiration and exudation of newly fixed C by primary producers and associated heterotrophs. Downstream changes in ^{13}C were monitored for up to 44 days to estimate the residence time and longer-term fate of autochthonous C. By tracing newly fixed C, we can better understand the fluxes and fate of autochthonous C in the context of freshwater ecosystem food webs and C cycling.

METHODS

Study site

We studied a 682-m reach of North Fork French Creek (hereafter, French Creek), a lake outlet stream in Medicine Bow National Forest, Wyoming, USA (41°19′46.84″ N, 106°21′32.61″ W). French Creek is a low-gradient, open-canopy stream in a subalpine forest meadow at 3115 m elevation (Fig. 1; see Plate 1). Average air temperature is 0.2°C with 1165 mm precipitation, most of which falls as snow (2002–2012 annual means from SNOTEL site 668; *available online*).[2] 2012 was a relatively warm and dry year with an annual mean temperature of 2.3°C and 757 mm precipitation. The dominant primary producer assemblages in French Creek are filamentous green algae, bryophytes, and biofilm on rocks. French Creek has low acid neutralizing capacity (ANC), and therefore low DIC. Using a low-slope reach for the $^{13}C_{DIC}$ addition reduced the amount

[2] http://www.wcc.nrcs.usda.gov/nwcc/site?sitenum=668&state=wy

of tracer lost to air-water gas exchange and low-ANC waters required less $^{13}C_{DIC}$ to enrich the total DIC pool compared to highly buffered streams.

To quantify physical properties of the stream reach, we estimated travel time (tt; s) and discharge (Q; m^3/s) using pulse additions of NaCl (Payn et al. 2009). Wetted width (w; m) was measured throughout our reach with a meter tape. We measured reach length (l; m) using a meter tape and GPS coordinates. Velocity (v; m/s) was calculated as l/tt. We estimated depth (z; m) based on continuity from v, Q, and w: $Q/(v \times w)$. Total reach travel time was 190 min. Mean Q, v, w, and z were 0.014 m^3/s, 0.06 m/s, 1.38 m, and 0.16 m, respectively, at the time of the tracer addition and were relatively stable throughout the study period.

Ecosystem metabolism

We compared ^{13}C fixation and fluxes with rates of gross primary production (GPP) and ecosystem respiration (ER), estimated via diel changes in dissolved oxygen (O_2), light, and temperature (T) for the upper and lower sections of our study reach. The upper and lower reaches were delineated by changes in channel morphology as the stream shifted from a higher-slope single channel reach to a lower-slope braided reach with small backwater pools and marshy areas. Hydrolab Minisondes (Hach, Loveland, Colorado, USA) recorded diel changes in O_2 and T at 10-min intervals (Δt; d) at the middle and bottom of our study reach.

We used a one-station, open-channel, metabolism model to estimate GPP, ER, and air–water gas exchange (following Hotchkiss and Hall [2014])

$$O_{2,(t)} = O_{2,(t-1)} + \left(\frac{GPP}{z} \times \frac{PPFD_{(t-1)}}{\sum PPFD_{24hr}}\right) + \frac{ER \times \Delta t}{z} + K_{O_2} \times \Delta t \times \left(O_{2sat,(t-1)} - O_{2,(t-1)}\right). \quad (1)$$

GPP and ER are positive and negative rates of O_2 production, respectively ($g \cdot O_2 \cdot m^{-2} \cdot d^{-1}$), K_{O_2} is temperature-corrected O_2 gas exchange rate (d^{-1}), and O_{2sat} is O_2 saturation concentration ($g\ O_2/m^3$). Photosynthetic photon flux density (PPFD; $\mu mol \cdot m^{-2} \cdot s^{-1}$) was modeled as in Hotchkiss and Hall (2014). There was minimal groundwater intrusion (measured with NaCl additions), so we did not include a groundwater correction term in our metabolism model.

We measured and modeled air–water gas exchange using additions of sulfur hexafluoride (SF_6; Wanninkhof 1992) and slope of nighttime O_2 rate of change vs. saturation deficit (nighttime regression method, possible for the lower reach only; Hornberger and Kelly 1975). Triplicate SF_6 samples were collected from nine sites along the 682-m reach during two daytime plateau releases and were analyzed on a gas chromatograph with an electron capture detector (Shimadzu GC-14A; Shimadzu, Kyoto, Japan). We used Schmidt number scaling to standardize SF_6 exchange to a Schmidt number of 600 (K_{600}; d^{-1}) and K_{O_2} (Wanninkhof 1992).

Posterior probability distributions of GPP, ER, and K_{600} were simulated using Bayesian parameter estimation via a random walk Metropolis algorithm and Markov chain Monte Carlo (MCMC) with the R *metrop* function in the *mcmc* package (R Development Core Team 2012, Geyer and Johnson 2013, Hotchkiss and Hall 2014). Prior information about K_{600} from SF_6 and nighttime regressions informed posterior model estimates of K_{600}. We weighted upper and lower reach GPP and ER by stream length to estimate whole-reach GPP and ER for comparisons with C fixation and flux estimates from whole-reach ^{13}C calculations (see Eq. 11).

$^{13}C_{DIC}$ tracer addition

The tracer experiment was conducted as a pulse-chase addition. Because we wanted to maximize algal fixation of the $^{13}C_{DIC}$ added, we limited our tracer addition to peak daylight on 30 and 31 August 2012 (hereafter referred to as days 0a and 0b, respectively). The isotope additions lasted 4 h each day to ensure $^{13}C_{DIC}$ moved through the entire 3-h travel time reach during daylight. By adding $^{13}C_{DIC}$ over 2 d, we maximized the isotope label in the algae without increasing DIC far above tracer levels. We steadily pumped 100 g of predissolved $^{13}C_{DIC}$ (98 atom % ^{13}C-$NaH^{13}CO_3$, Sigma-Aldrich, St. Louis, Missouri, USA) over 2 d using approaches developed for ^{15}N (Hall et al. 2009; others). The pH of the $^{13}C_{DIC}$ solution was increased to 9.7 using NaOH to limit conversion of tracer to CO_2 and loss to the atmosphere before addition to the stream. Target $^{13}C_{DIC}$ stream water enrichment was 1000‰, which increased total DIC < 10%.

Sampling ^{13}C of stream C pools

We monitored changes in $^{13}C_{DIC}$, $^{13}C_{DOC}$, and particulate OC pools ($^{13}C_{POC}$) at nine stations downstream of the release before, during, and for up to 44 d after the tracer addition. Preenrichment samples were collected for DIC, DOC, suspended POC (sPOC), fine benthic POC (fbPOC), biofilm on rocks, filamentous algae, and bryophytes (sampling methods similar to Hall et al. 2009). We collected site-specific duplicate DIC and DOC samples; sPOC and benthic OC were combined into a single sample for each pool at each site. Concentrations and ^{13}C of all C pools were monitored at one location upstream of the tracer addition site before and after the release to control for any natural changes in ^{13}C over time (none detected). All isotope samples were analyzed at the University of Wyoming Stable Isotope Facility in Laramie, Wyoming, USA.

DOC and DIC were sampled during the two days of tracer addition (0a, 0b), in the morning and afternoon of day 1 after the addition (1am, 1pm), and then on days 2, 3, 4, 6, 9, 11, and 16. We collected $^{13}C_{DIC}$ samples in airtight glass Wheaton vials (Wheaton Industries, Mill-

ville, New Jersey, USA) with 200 μL supersaturated $HgCl_2$ to stop biological activity before analysis with a Thermo Gasbench coupled to a Thermo Delta Plus XL IRMS (Thermo Fisher Scientific, Waltham, Massachusetts, USA). DIC concentrations were estimated using acid neutralizing capacity (mmol/L) and pH (as in Hotchkiss and Hall [2010]). We filtered DOC samples through ashed Whatman GF/F filters (GE Healthcare Life Sciences, Pittsburg, Pennsylvania, USA) into ashed borosilicate vials. DOC samples were acidified with HCl to a target pH of 2 and refrigerated immediately after collection. We measured DOC concentrations on a Shimadzu TOC Analyzer (TOC-500A; measurement precision ±0.05 mg C/L; Shimadzu, Kyoto, Japan). To analyze $^{13}C_{DOC}$, we used offline chemical oxidation to convert DOC to DIC for $^{13}C_{DIC}$ analyses. For this, we added 4 mL of acidified DOC sample and 1 mL potassium persulfate solution to preashed 12-mL Labco borosilicate Exetainer vials (Labco, Lempeter, Ceredigion, UK; Lang et al. 2011). The vials were sealed and flushed with high-purity helium gas (60 mL/min for 10 min) to remove DIC from the sample (Lang et al. 2011). To oxidize DOC to DIC, we heated vials in 92°C water baths for 2 h (adapted from Lang et al. [2011] for lower boiling points at higher elevation in Laramie, Wyoming, USA). Samples of ultrapure water (Milli-Q Plus; EMD Millipore, Billerica, Massachusetts, USA) were included as DOC-free controls to confirm removal of background DIC. We also spiked replicate vials of ultrapure water with a known DOC concentration to confirm recovery of spiked DOC as headspace CO_2. Samples were cooled before analyzing for $^{13}C_{DIC}$ with a Thermo Gasbench coupled to a Thermo Delta Plus XL IRMS.

To trace C fixed in primary producer biomass, we inventoried tracer ^{13}C in OC pools on days 1, 3, 6, 9, 16, 23, 30, and 44. All $^{13}C_{POC}$ samples were acidified with 2 mol/L HCl to remove $H^{13}CO_3$, rinsed three times with ultrapure water, dried, and homogenized before analysis with a Costech 4010 Elemental Analyzer (Costech Analytical Technologies, Valencia, California, USA) coupled to a Thermo Delta Plus XP IRMS. We measured $^{13}C_{POC}$ and ash-free dry mass (AFDM; g C/m^2) of OC samples: sPOC, fbPOC, and biofilm, algal, and bryophyte assemblages. Biofilm samples were collected by scrubbing biofilm off rocks, measuring rock area by tracing, and subsampling the biofilm slurry for AFDM and $^{13}C_{biofilm}$ on GF/F filters. We estimated fbPOC ^{13}C and AFDM by subsampling and filtering fbPOC stirred up from the benthos in a stovepipe of known diameter and water depth at each site. We filtered a known amount of water through replicate GF/F filters to collect sPOC AFDM and $^{13}C_{sPOC}$ samples. Grab samples for $^{13}C_{algae}$ and $^{13}C_{bryo}$ at each site were homogenized before analyses. Triplicate algal and bryophyte AFDM samples were collected using a large-diameter stovepipe from lower, mid, and upper parts of French Creek during the middle of the 44-d sampling period.

Modeling ^{13}C fluxes and fate

We used changes in the ^{13}C signature of DOC, DIC, and particulate OC to trace the fate of newly fixed C in French Creek (see Table 1 for a summary of data and assumptions needed for each parameter). All ^{13}C pools are in units of g ^{13}C of added tracer for model estimates. Isotope data were transformed from $\delta^{13}C$ (‰) to atom fraction (F; ^{13}C/total C) of enriched (F_{enr}) and natural abundance (F_{nat}) samples. We calculated mass of ^{13}C from F_{xs} ($F_{xs} = F_{enr} - F_{nat}$) and the concentrations of C pools, [C]

$$\text{mass } ^{13}C = F_{xs} \times [C]. \quad (2)$$

$^{13}C_{DIC}$, $^{13}C_{DOC}$, and $^{13}C_{sPOC}$ concentration units were g ^{13}C/m^3, while ^{13}C of primary producer pools and $^{13}C_{fbPOC}$ was modeled as g ^{13}C/m^2.

We estimated total $^{13}C_{DIC}$ removal from the water column during our tracer addition, where removal was the sum of $^{13}C_{DIC}$ fixation by primary producers and outgassing to the atmosphere. The net DIC removal rate (k_{DIC}; m^{-1}) was estimated using downstream changes in $^{13}C_{DIC}$ fluxes (g ^{13}C/d) from the release site (x; m)

$$^{13}C_{DIC} = {}^{13}C_{DIC(0)} e^{-k_{DIC}x}. \quad (3)$$

To solve for k_{DIC}, $^{13}C_{DIC}$ fluxes (g ^{13}C/d) were calculated as

$$^{13}C_{DIC} = F_{xs} \times Q \times [C]. \quad (4)$$

Water column DIC concentrations (g C/m^3) are represented by [C]. We used nonlinear least squares in R (nls; R Development Core Team 2012) to solve for k_{DIC} and $^{13}C_{DIC(0)}$ (g $^{13}C_{DIC}$/d at the release site; Johnson et al. 2013) as unknown parameters in an exponential function (Eq. 3). We calculated total tracer removed and scaled to total release time.

Dynamic two-compartment flux models (Wollheim et al. 2001, Johnson et al. 2013) were used to quantify net autochthonous DOC exudation (k_{exud}; d^{-1}) given DOC uptake (k_{upt}; m^{-1}), biomass decline in ^{13}C (k_{loss}; m^{-1}), $^{13}C_{DOC}$ flux (DO^{13}C; g ^{13}C/d), and the isotope tracer in primary producer biomass at each sampling station (PP scaled by wetted width; g ^{13}C/m)

$$\frac{d\text{DO}^{13}\text{C}}{dx} = k_{exud} \times \text{PP} - k_{upt} \times \text{DO}^{13}\text{C} \quad (5)$$

$$\frac{d\text{PP}}{dx} = -k_{loss} \times \text{PP}. \quad (6a)$$

We solved Eq. 6a as

$$\text{PP}_x = \text{PP}_0 e^{-k_{loss}x}. \quad (6b)$$

We estimated k_{loss} and PP_0 on days 0b, 1 (am and pm), 3, and 6 using linear regression of ln transformed Eq. 6b. PP_x values used to estimate the intercept for ^{13}C in primary producer biomass (PP_0) on the second release day (0b) and day 1 were all from day 1 benthic samples,

TABLE 1. Data, assumptions, and equations required to calculate and model key fluxes and fates of ^{13}C and total C.

Parameter	Description	Units	Eqs.	Data and assumptions required
GPP	gross primary production	g C·m^{-2}·d^{-1}	1	Model requires light, temperature, and O_2.
ER	ecosystem respiration	g C·m^{-2}·d^{-1}	1	Conversion to g C from g O_2 assumes a 1:1 molar ratio of CO_2 fixed : O_2 produced (for GPP) or CO_2 produced : O_2 consumed (for ER)
mass ^{13}C	mass of ^{13}C in a pool of interest	g $^{13}C/m^2$ or g $^{13}C/m^3$	2	For the pool of interest: calculation requires concentration of total C pool, as well as the natural abundance and enriched atomic fractions.
k_{DIC}	rate of abiotic + biotic ^{13}C removal from water column (dissolved inorganic carbon)	m^{-1}	3, 4	Modeling requires $^{13}C_{DIC}$ fluxes during the tracer addition at stations downstream of release (calculated using Eq. 4). $^{13}C_{DIC}$ flux vs. distance downstream data should match linear or nonlinear model used to solve for k_{DIC}.
k_{upt}	rate of dissolved organic carbon (DOC) uptake	m^{-1}	5, 7	Assumed to be zero, resulting in a conservative estimate of k_{exud}.
k_{loss}	rate of biomass decline in ^{13}C	m^{-1}	6a, 6b, 7	Modeling requires g ^{13}C in primary producer biomass scaled to wetted width (PP; g ^{13}C/m) at known sites downstream of tracer addition. PP versus distance downstream data should match linear or nonlinear model used to estimate slope (k_{loss}) and intercept (PP_0).
PP_0	^{13}C in upstream autotrophs	g ^{13}C/m	6a, 6b, 7	
k_{exud}	net rate of DOC exudation of newly fixed C	d^{-1}	5, 7	Modeling requires $^{13}C_{DOC}$ flux, k_{upt}, k_{loss}, and PP_0. k_{exud} is estimated by decreasing the difference between measured and modeled $^{13}C_{DOC}$ flux with nlm. Assume $k_{upt} = 0$ if no independent measurement.
k_{newR}	net respiration rate of newly fixed C	d^{-1}	8, 9	Modeling requires $^{13}C_{DIC}$ flux, k_{DIC}, k_{loss}, and PP_0. k_{newR} is estimated by decreasing the difference between measured and modeled $^{13}C_{DIC}$ flux with nlm. k_{DIC} was measured during the tracer addition.
C fixed	net C fixed into autotrophs	g C/m^2	10	Calculation requires g ^{13}C of autotrophic biomass, DIC, and g C_{DIC}. Scale-up C fixed at each site to compare with reach-scale GPP.
aPP	actively fixing autotroph biomass	g C/m^2	11	Calculation requires GPP, C fixed, k_{exud}, and k_{newR}. In addition to the assumptions for all parameters in Eq. 11, assume difference between GPP and C fixed is from exudation and respiration of newly fixed C.
$Flux_{DOC}$	Autochthonous DOC flux	g C·m^{-2}·d^{-1}	$k_{exud} \times$ aPP	These net DOC and DIC flux calculations are a function of all assumptions required to estimate aPP and k_{exud} or k_{newR}.
$Flux_{DIC}$	Autochthonous DIC flux	g C·m^{-2}·d^{-1}	$k_{newR} \times$ aPP	

because we did not sample benthic pools during the tracer release. We combined Eq. 5 and 6b and solved the differential equation (as in Wollheim et al. [2001] and Johnson et al. [2013])

$$DO^{13}C = \frac{k_{exud} \times PP_0}{k_{upt} - k_{loss}} \times (e^{-k_{loss} \times x} - e^{-k_{upt} \times x}). \quad (7)$$

We solved for k_{exud} using estimates of PP_0 and k_{loss} from Eq. 6b. Nonlinear minimization in R (nlm; R Development Core Team 2012) was used to estimate k_{exud} by minimizing the –log likelihood of $DO^{13}C$ given modeled k_{exud} (Hilborn and Mangel 1997). We used a likelihood ratio test to estimate confidence intervals for k_{exud} (Hilborn and Mangel 1997). To avoid equifinality among parameters, we did not solve for both k_{exud} and k_{upt}, and instead assumed no uptake of DOC ($k_{upt} = 0$; Johnson et al. 2013). No uptake is unlikely given the high biological availability of autochthonous DOC, so estimates of autochthonously produced DOC fluxes are therefore conservative.

We modeled net respiration of newly fixed C, k_{newR} (d^{-1}), using the same framework and equations as for k_{exud}, where Eq. 5 becomes

$$\frac{dDI^{13}C}{dx} = k_{newR} \times PP - k_{DIC} \times DI^{13}C \quad (8)$$

and is combined with Eq. 6b to estimate k_{newR} (using k_{DIC} from Eq. 3) where

$$DI^{13}C = \frac{k_{newR} \times PP_0}{k_{DIC} - k_{loss}} \times (e^{-k_{loss} \times x} - e^{-k_{DIC} \times x}). \quad (9)$$

Tracer ^{13}C mass and turnover rates were quantified for each benthic OC pool. We calculated turnover rates (k_{turn}; d^{-1}) for each OC pool at each site as the slope of log-transformed mass of ^{13}C tracer vs. time. An average turnover rate of each pool was estimated from the mean of all sites. We also measured export of $^{13}C_{DOC}$, $^{13}C_{DIC}$, and $^{13}C_{sPOC}$ after the tracer release. Export fluxes were calculated as in Eq. 2 and scaled up to per day rates of g ^{13}C exported downstream.

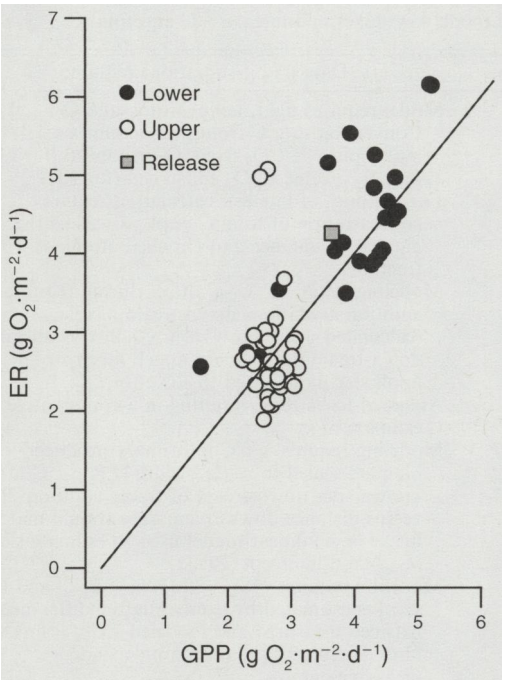

FIG. 2. Estimates of gross primary production (GPP; positive rates) and ecosystem respiration (ER; absolute value of negative rates) in the upper and lower reaches of French Creek. Release is the reach-scale average GPP and ER estimated from O_2 during the tracer addition. The line is a 1:1 line.

We estimated the net mass of C fixed (g C/m^2) into primary producer biomass as

$$\text{C fixed} = \frac{\text{g } C_{DIC} \times \text{g } {}^{13}C_{Biomass}}{\text{g } {}^{13}C_{DIC}}. \quad (10)$$

We calculated net C fixed for each site 1 d after the addition and for the whole reach by scaling from each site. We scaled mass of C fixed to a daily flux (g C·m^{-2}·d^{-1}) by dividing by 8 h (4 h of tracer addition during 2 d). We converted whole-reach GPP and ER during the tracer addition, as modeled from O_2 production (Eq. 1), to g C·m^{-2}·d^{-1} for comparison with C fixed (assuming a 1:1 ratio of moles O_2 produced to CO_2 fixed).

To calculate whole-stream fluxes of C from ^{13}C, we needed to know the biomass of actively fixing primary producers. Because we could only directly measure the total biomass of primary producer assemblages and not the mass of actively fixing primary producers (aPP; g C/m^2), we used GPP and C fixed to estimate aPP (similar to Johnson et al. [2013]),

$$\text{C fixed} = \text{GPP} - k_{exud} \times \text{aPP} - k_{newR} \times \text{aPP}. \quad (11)$$

This estimate is a lower bound because aPP should be higher than the amount of C fixed in 24 h (GPP). GPP was our measurement of total C fixed, so the difference between GPP and C fixed was any newly fixed C lost to exudation or respiration before we sampled primary producer biomass for ^{13}C on day 1. We used aPP to calculate conservative whole-stream fluxes of DOC ($\text{Flux}_{DOC} = k_{exud} \times \text{aPP}$) and DIC ($\text{Flux}_{DIC} = k_{newR} \times \text{aPP}$) from newly fixed C 1 d after the tracer addition and compared these fluxes of new autotrophic C to GPP and ER.

RESULTS

Ecosystem metabolism

Gross primary production (GPP) drove ecosystem respiration (ER) in French Creek (Fig. 2). Paired daily rates of GPP and ER were nearly balanced and mirrored each other in both the upper and lower reach throughout the study period (Fig. 2; Appendix A). GPP and ER were higher and more variable in the lower than the upper reach (Fig. 2). Mean and standard deviation (±SD) of GPP was 2.7 ± 0.2 in the upper reach and 4.0 ± 0.9 g O_2·m^{-2}·d^{-1} in the lower reach. ER in the upper and lower reach was −2.7 ± 0.7 and −4.3 ± 1.0 g O_2·m^{-2}·d^{-1}, respectively. Net ecosystem production (NEP; GPP + ER) was 0.0 ± 0.7 and −0.3 ± 0.6 g O_2·m^{-2}·d^{-1} in the upper and lower reaches during the study. Whole-reach (upper and lower combined) GPP and ER during the tracer release were 3.7 and −4.3 g O_2·m^{-2}·d^{-1}, respectively (Fig. 2). Converted to g C, whole-reach GPP and ER during the tracer addition were 1.4 and −1.6 g C·m^{-2}·d^{-1}.

$^{13}C_{DIC}$ tracer addition and removal

We enriched stream $^{13}C_{DIC}$ by approximately 1500‰ during two consecutive 4-h daytime tracer releases (Appendix B). Measured DIC fluxes during the release ranged from 57.6 to 9.6 g ^{13}C/d at the upper and lower ends of the study reach (Fig. 3). Linear model estimates and 95% confidence intervals (lower, upper) of DIC flux at 0 m (y intercept) were 56.4 (46.9, 66.1) and 56.9 (53.7, 59.9) g ^{13}C/d on release days 0a and 0b. These fluxes at 0 m scaled to 18.89 g ^{13}C added during our two 4-h tracer releases. We added a total of 15.3 g ^{13}C, so higher linear model estimates of g ^{13}C at 0 m may be due to incomplete mixing of tracer, error in measuring discharge at the upper measurement sites (25, 48, and 120 m), or error in estimating the y intercept from downstream DIC fluxes. We used the known amount of tracer added (1.91 g ^{13}C/h for 2 4-h releases) to estimate g ^{13}C tracer removed within the reach due to biological fixation, outgassing to the atmosphere, and export downstream.

We accounted for 95% of tracer ^{13}C added through measurements of fixation, release, and export during and after the addition. Biological C fixation and outgassing of $^{13}C_{DIC}$ to the atmosphere removed most of the $^{13}C_{DIC}$ from the water as the tracer flowed through the study reach. We used the decline in DIC downstream of the release site to estimate whole-reach rates of DIC removal (k_{DIC}) and total g $^{13}C_{DIC}$ removed (Fig. 3). Estimates of k_{DIC} on days 0a and 0b were 0.0023 and 0.0024/m, respectively. 10.6 g $^{13}C_{DIC}$ were removed from the study reach due to both fixation and loss to the atmosphere during the two release days,

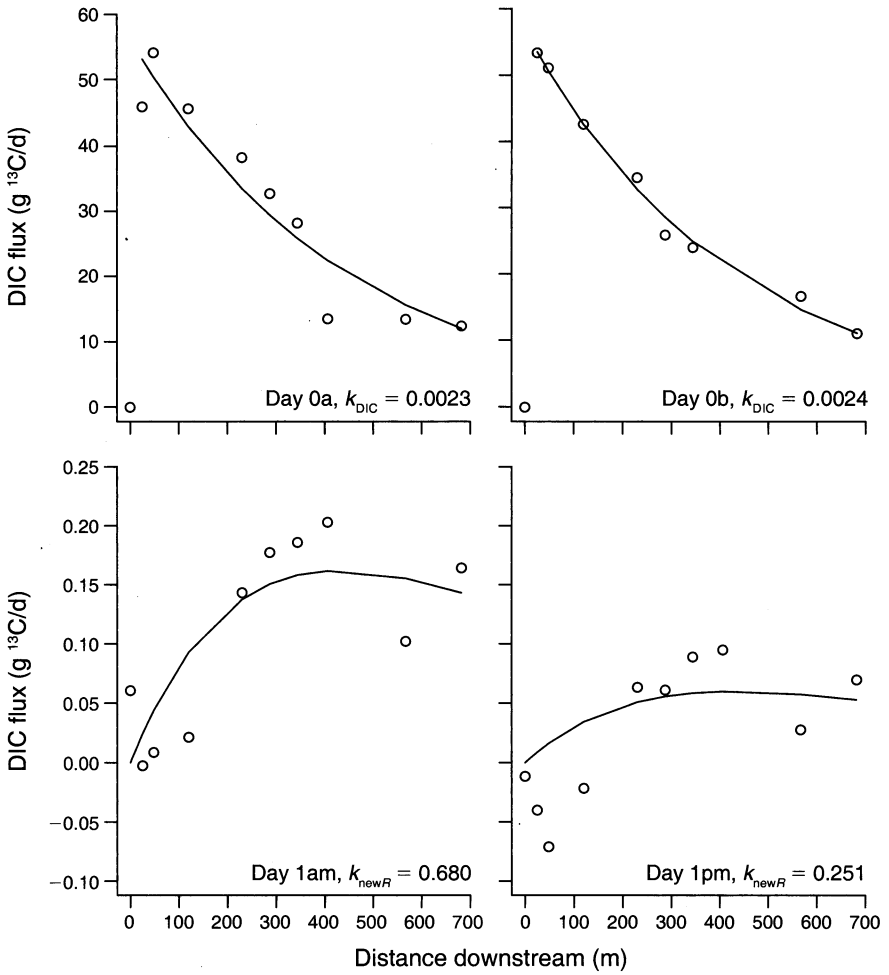

FIG. 3. Measured and modeled tracer $^{13}C_{DIC}$ (^{13}C from dissolved inorganic carbon) downstream of the tracer release site during (day 0a and day 0b; top panels) and after (day 1am and day 1pm; bottom panels) the $^{13}C_{DIC}$ tracer addition. Days 0a and 0b represent the two tracer addition days on 30 and 31 August 2012, respectively. Measured $^{13}C_{DIC}$ fluxes are open circles; modeled $^{13}C_{DIC}$ flux is the solid line. Tracer $^{13}C_{DIC}$ declined downstream of the release site due to biological uptake and outgassing to the atmosphere. Model estimates of k_{DIC} (rate of removal of $^{13}C_{DIC}$ from the water column; Eq. 3) were 0.0023 and 0.0024 m^{-1} and modeled fluxes of $^{13}C_{DIC}$ at the release site (y-intercept) were 2.35 and 2.37 g ^{13}C/h. $^{13}C_{DIC}$ increased downstream of the tracer release site on day 1 after the $^{13}C_{DIC}$ tracer addition, likely due to respiration of newly fixed ^{13}C. $^{13}C_{DIC}$ production on day 1 was modeled using estimates of k_{newR} (net respiration of newly fixed C; d^{-1}) from Eqs. 8 and 9 and average k_{DIC}. See Table 3 for model parameter estimates, likelihoods, and confidence intervals.

which was 69% of the tracer added (Table 2). Total tracer export from the bottom of the study reach during the 2-d release period was 3.9 g ^{13}C (Table 2). Combined estimates of tracer removal and tracer export were 14.5 g ^{13}C, leaving only 0.8 g ^{13}C unaccounted for by our budgeting calculations.

Stream $^{13}C_{DIC}$ was enriched 1 d after the tracer addition, with modeled $^{13}C_{DIC}$ production rates (k_{newR}) of 0.680 and 0.251/d in the morning and afternoon of day 1, respectively (Table 3; Fig. 3). Stream $^{13}C_{DIC}$ returned to near-background levels after day 1 (Fig. 3; Appendix B). Following Johnson et al. (2013), we estimated the biomass of actively fixing primary producers (aPP) using GPP, net C fixed from tracer ^{13}C in benthic OC, and modeled DOC and DIC production (Eq. 11). aPP was 0.5 g C/m^2, which was only 7.7% of the mean total standing stock of biofilm, algae, bryophytes, and associated heterotrophs (6.5 g C/m^2). Low aPP was driven by high k_{newR} the morning after the tracer addition. If DIC production from respiration of newly fixed C were lower at 0.2/d (as in the afternoon of day 1), aPP would be 1.2 g C/m^2, which is closer to 20% of total biomass of primary producers and associated heterotrophs measured in French Creek.

Release as $^{13}C_{DOC}$

Primary producers and associated heterotrophs rapidly turned over their newly fixed C by releasing DOC into the water column at rates of up to 16% per d (Table 3; Fig. 4). Rates of net autochthonous DOC release

TABLE 2. Fate of newly fixed C during and after the ^{13}C tracer addition.

C pool	^{13}C fixed by day 1 (g ^{13}C/reach)	^{13}C turnover (d^{-1} over 44d)	^{13}C residence time (d)	^{13}C export during release (g ^{13}C/2 d)	^{13}C export after release (g ^{13}C/6 d)
Algae	0.067	0.0203	49		
Biofilm	0.620	0.0172	58		
Bryophytes	0.044	0.0131	76		
fbPOC	0.057	0.0087	114		
sPOC				0.018	0.354
DOC				0.018	0.029
DIC	10.58†			3.928	0.375
Pool average		0.0162	62		
Total OC	0.788			0.036	0.758

Notes: We calculated export flux using Eq. 6b and interpolated between sampling days to obtain estimates for up to 6 d after the tracer addition. fbPOC, sPOC, DOC, and DIC represent fine benthic particulate organic C, suspended POC, dissolved OC, and dissolved inorganic C, respectively.

† DIC fixed accounts for all ^{13}C removal from the water column during the tracer release (biological fixation as well as outgassing to the atmosphere).

(k_{exud}), measured using tracer ^{13}C enrichment of primary producer biomass and water column DOC (Eqs. 5–7), were highest during and immediately after the tracer addition and declined to 1% per d by day 6 (Table 3; Fig. 4). Tracer $^{13}C_{DOC}$ exudation on day 1 after the tracer addition was higher in late afternoon (1pm) than early morning (1am). $^{13}C_{DOC}$ flux estimates were more variable than other C pools and modeled k_{exud} had wide confidence intervals as a result (Table 3). Assuming k_{exud} of 0.16/d and aPP of 0.5 g C/m^2, newly fixed C was released as DOC at 0.08 g C·m^{-2}·d^{-1} during the tracer addition. Measurable $^{13}C_{DOC}$ was low (Table 2), but we did see downstream declines in $^{13}C_{DOC}$ on several days (Fig. 4), which suggests our assumption of no $^{13}C_{DOC}$ uptake to solve for DOC production gave modeled net k_{exud} estimates that were lower than actual rates of DOC exudation in French Creek.

Storage and turnover of fixed $^{13}C_{DIC}$

Net C fixed measured via ^{13}C incorporation (Eq. 10) was 0.98 and 0.93 g C·m^{-2}·d^{-1} on release days 0a and 0b, respectively, which accounted for 68–72% of whole-reach GPP modeled using O_2. All benthic pools were enriched with ^{13}C 1 d after the tracer release (Table 2; Fig. 5; Appendix C). We found 0.79 g ^{13}C in benthic pools on day 1 after the tracer addition (Table 2; Appendix C). Biofilm fixed 79% of the tracer found in benthic OC on day 1 (Table 2; Appendix C). Algae, bryophytes, and fbPOC pools incorporated 8.5%, 7.2%, and 5.6% of the tracer found in total benthic OC (Table 2; Appendix C).

After the initial rapid turnover, tracer ^{13}C in benthic POC declined to 20% of original enrichment after 44 d (Fig. 5; Appendix C). Biofilm still had the most ^{13}C: 14.3% compared to 3.1%, 1.5%, and 1.1% in bryophytes, fbPOC, and algae, respectively (Fig. 5; Appendix C). Residence times calculated from turnover rates ($1/k_{turn}$; d) for the 44-d study period were lowest in algae, with a residence time of 49 d (Table 2; Fig. 5). Biofilms had a similar residence time as algae (58 d; Table 2; Fig. 5). Bryophyte and fbPOC residence times were 76 and 114 d, respectively (Table 2; Fig. 5). High reach-scale biofilm biomass (5 g C/m^2) relative to algae (0.3 g C/m^2), bryophytes (1.2 g C/m^2), and fbPOC (2.8 g C/m^2), coupled with higher ^{13}C fixation and lower residence time than other benthic pools, suggests biofilm dominated autochthonous C cycling in French Creek during this period.

DISCUSSION

The rich history of C cycling research in freshwater ecosystems has focused largely on the processing and fate of terrestrial organic matter (Fisher and Likens 1973, Webster 2007, Lapierre et al. 2013) and how these subsidies influence food webs (Wallace et al. 1997, Carpenter et al. 2005, Marcarelli et al. 2011). Despite the

TABLE 3. Model parameters used to estimate $^{13}C_{DOC}$ and $^{13}C_{DIC}$ fluxes.

Day	PP_0(g ^{13}C/m)	k_{loss}(m^{-1})	k_{exud}(d^{-1})	CI_{lower}	CI_{upper}	−LL	k_{newR}(d^{-1})	CI_{lower}	CI_{upper}	−LL
0b	0.0015	0.002	0.159	0.048	0.276	−15.0	...	...	...	...
1am	0.0015	0.002	0.044	0.014	0.075	−28.7	0.680	0.520	0.839	−17.7
1pm	0.0015	0.002	0.092	0.004	0.180	−18.1	0.251	0.083	0.420	−17.8
3	0.0014	0.006	0.016	−0.019	0.061	−34.4	...	...	...	...
6	0.0011	0.003	0.011	−0.031	0.053	−30.2	...	...	...	...

Notes: Intercept for ^{13}C in primary producer biomass on day 0 (PP_0), rate of biomass decline in ^{13}C downstream (k_{loss}), rate of autochthonous dissolved organic carbon (DOC) exudation (k_{exud}), and rate of dissolved inorganic carbon (DIC) added to the water column on day 1 due to respiration of newly fixed C (k_{newR}). Dates include the second release day (0b), the morning and afternoon of day 1 (1am, 1pm), day 3, and day 6 after the $^{13}C_{DIC}$ tracer release. We calculated PP_0 and k_{loss} from Eq. 6b. We modeled k_{exud} and k_{newR} using Eqs. 7 and 10 and nonlinear minimization to minimize the negative log likelihood (−LL) of modeled k_{exud} or k_{newR}, and a likelihood ratio test to estimate k confidence intervals (CI). Ellipses mean no data.

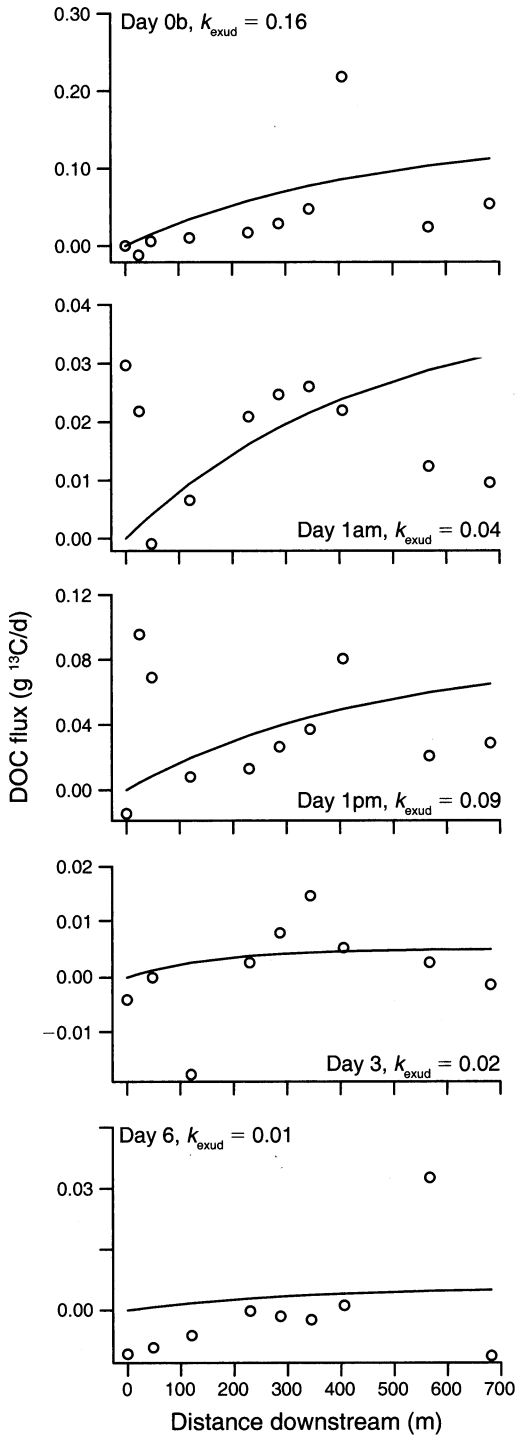

FIG. 4. Measured and modeled $^{13}C_{DOC}$ (dissolved organic carbon) downstream of the tracer release site during (day 0b) and after (day 1am, day 1pm, day 3, and day 6) the $^{13}C_{DIC}$ tracer addition. Measured $^{13}C_{DOC}$ fluxes are open circles; modeled $^{13}C_{DOC}$ flux is the solid line. Note the different y-axis ranges. $^{13}C_{DOC}$ fluxes were modeled using Eqs. 5–7. The release rates for k_{exud} are d^{-1}. See Table 3 for model parameter estimates, likelihoods, and confidence intervals.

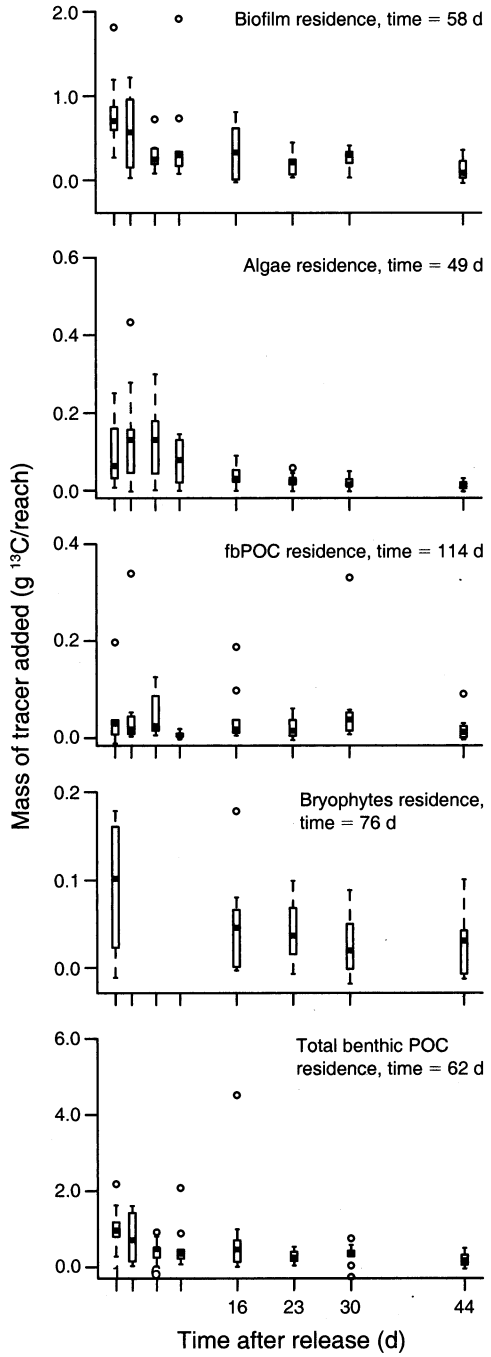

FIG. 5. The amount of $^{13}C_{DIC}$ in benthic particulate organic C (POC) from 1 to 44 d after the tracer addition. Total benthic POC is the sum of all measured benthic OC pools: biofilm, algae, fbPOC (fine benthic POC), and bryophytes. Whiskers represent the minimum and maximum values for g ^{13}C averaged among all nine sites, points are outliers, boxes range from the first and third quartile, and the thick line within the box represents the median ^{13}C of each benthic C pool on that sampling day. Pool residence time was calculated using turnover data from day 1 through day 44, where residence time is $1/k_{turn}$ (d; where k_{turn} is the turnover rate).

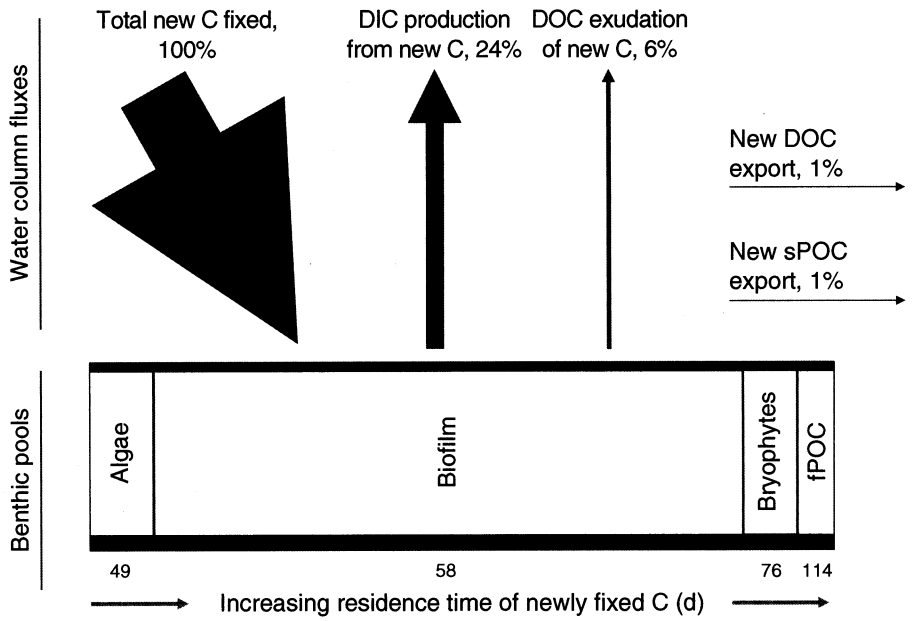

FIG. 6. Short-term fluxes and longer-term residence time of newly fixed carbon (C) in French Creek, Wyoming, USA. Flux arrows are scaled relative to the percentage of total new C incorporation in 1 d as estimated by gross primary production (GPP; Fig. 2), with each daily flux as a percentage of GPP. Short-term fluxes were estimated during and 1 d after the $^{13}C_{DIC}$ tracer addition (days 0b and 1). Dissolved inorganic C (DIC) production and dissolved organic C (DOC) exudation are net fluxes. Suspended particulate OC (sPOC) and DOC export were measured at the bottom of the study reach. Benthic pools (fine particulate organic C [fPOC], bryophytes, biofilm, and algae) are scaled to the percentage of ^{13}C tracer found in each pool on day 1 and ordered from left to right based on shortest to longest residence time of newly fixed C (Fig. 5). The flux arrow widths and benthic pool sizes are presented at different scales (percentage of 1 d GPP vs. percentage of ^{13}C incorporation) to visualize the smallest fluxes and largest pools in the same diagram.

longstanding appreciation that autochthonous C can fuel food webs, we know less about how primary production contributes to C cycling in running waters, including the capacity of autochthonous C to influence DIC dynamics and the timescales over which newly fixed C turns over in different C pools. Using tracer methods, we showed that much of GPP turned over rapidly, potentially fueling heterotrophic production through the immediate release of biologically available DOC. Only 20% of newly fixed autochthonous C remained in the study reach OC pools 44 d after the tracer addition.

$^{13}C_{DIC}$ release after fixation

Tracer ^{13}C in the benthos turned over quickly in French Creek, with 30% of GPP released as DOC and DIC shortly after fixation (Fig. 6). Enrichment of DIC on day 1 was likely solely due to respiration of fixed ^{13}C. Because reach travel time was four times shorter than the time between the end of the release and the DIC measurements the next morning, it is unlikely that there was any tracer left in the reach. Calculated net DIC production from newly fixed C was 24% of GPP, suggesting nearly one quarter of recently fixed OC supported the respiration of primary producers and associated heterotrophs (Fig. 6). This value is somewhat lower than modeled respiration of newly fixed C (ERa), which was 44% of GPP for a range of streams (Hall and Beaulieu 2013). While CO_2 production from newly fixed autotrophic C may not play a role in net C emissions over longer spatial and time scales (CO_2 fixed by primary producers is eventually respired back into the water column if not buried as OC), the timing and location of GPP-derived CO_2 production has the potential to drive smaller-scale C dynamics, support internal primary production, and influence CO_2 efflux measurements. GPP and ER in French Creek were relatively balanced during our study, but comparisons of ER and fluxes of DIC from newly fixed C implied that much of ER was of upstream OC and older autochthonous C. Although we could model the net rates of ^{13}C release after fixation, calculating the net fluxes of whole-stream DIC production and DOC exudation relative to GPP and ER is more difficult because fluxes of newly fixed C are the product of k_{newR} or k_{exud} and the biomass of primary producers that are actively fixing C (aPP), which is not the same as total primary producer biomass in the stream and not an easily measureable quantity.

Autochthonous $^{13}C_{DOC}$ exudation

Algae released a substantial proportion of fixed C as DOC soon after fixation. It is well known from mesocosm, lake, and marine tracer studies that algae release some fraction of fixed C as DOC; here we provide empirical estimates of net autochthonous DOC exudation at the stream reach scale. Autochthonous DOC can fuel heterotrophic production, but is difficult

PLATE 1. Lower reach of French Creek, Medicine Bow National Forest, Wyoming, USA. Photo credit: E. R. Hotchkiss.

to quantify because of the rapid DOC consumption by microbes that is tightly coupled with C release from primary producers (Cole et al. 1982). Newly fixed C was released at a net rate of 0.16/d while primary producers were fixing $^{13}C_{DIC}$ during the tracer addition. An increase in autochthonous DOC exudation during the day would explain higher net release rates in the afternoon, which has been hypothesized to fuel higher daytime heterotrophic respiration compared to nighttime (Tobias et al. 2007, Hotchkiss and Hall 2014). The tight coupling between GPP and ER measured throughout the study period also supports the role of GPP and associated DOC exudation in driving both autotrophic and heterotrophic respiration in French Creek. DOC exudation seemed to be more of a short-term fate for newly fixed C, because estimates of k_{exud} declined to near zero by day 6.

Whole-stream DOC release of newly fixed C was at least 6% of GPP (Fig. 6). Modeled DOC exudation from a short-term $^{13}C_{DIC}$ addition does not include exudation of older autochthonous C, only recently fixed C. Net newly fixed DOC exudation was within the range of literature estimates from other habitats and methods, where previous estimates of autochthonous DOC production rates, as a percent of GPP, range from 3–42%, with a mean of ~13% (Baines and Pace 1991, Bade et al. 2007, Lyon and Ziegler 2009). As with DIC production, our estimate of whole-stream net DOC release is a conservative one and is partly driven by low calculated mass of aPP. If aPP were 20% of the mean standing stock of biofilm, algae, bryophytes, and associated heterotrophs, DOC exudation fluxes would be closer to the reviewed mean for aquatic ecosystems at 14% of GPP. Primary producers exude older C in addition to fixed C (Lyon and Ziegler 2009), which we could not account for with a short-term tracer addition, but may also provide highly bioavailable C for heterotrophic production and respiration in streams.

We found evidence for the release of newly fixed C as $^{13}C_{DOC}$, but the measured net enrichment of $^{13}C_{DOC}$ in the water column was a fraction of the total autochthonous $^{13}C_{DOC}$ released. We emphasize that we quantified net $^{13}C_{DOC}$ release, which is lower than gross rates of $^{13}C_{DOC}$ released by primary producers, because we assumed no $^{13}C_{DOC}$ uptake. Thus, what we measured as net $^{13}C_{DOC}$ production was only the $^{13}C_{DOC}$ in the water column that was not already consumed by heterotrophs. Microbes may preferentially consume DOC of autochthonous origin, even in ecosystems with higher concentrations of terrestrial than autochthonous DOC (Kritzberg et al. 2005, Guillemette et al. 2013). We suspect gross release rates and fluxes of $^{13}C_{DOC}$ were higher than those we report for French Creek, and some of the autochthonous C budgeted as stored in benthic OC may have in fact been released, consumed, and retained.

Residence time and storage of ^{13}C

After short-term losses as DIC and DOC, up to 40% of ^{13}C fixed in primary producer biomass was exported as sPOC downstream of the study reach. Eighty percent of the ^{13}C fixed was no longer in benthic OC pools by day 44. Total residence time of autochthonous C varied among primary producers, with longer residence times

of ^{13}C in bryophytes relative to algae and biofilm (Fig. 6). While we refer to this fate of autochthonous C as storage, we note that the residence of newly fixed C in primary producer pools (49–76 d) was shorter than mean residence times of terrestrial organic material in forested headwater streams, which ranged from 102 d for leaves, 5.5 yr for sticks, and >8 yr for logs (Webster et al. 1999). Measured fbPOC had delayed maximum enrichment relative to the other benthic pools, likely because fbPOC was a mixture of some primary producers and mostly detritus. Newly fixed C in fbPOC had the longest residence time in French Creek at 114 d, but was shorter than 2.6 yr for bulk fbPOC estimates from headwater streams (Webster et al. 1999). Although we do not know the trajectory of autochthonous C turnover beyond our measurement at 44 d, fbPOC and bryophytes likely had slower turnover than algae and biofilm. We suspect that most tracer in algae and biofilm did not persist through winter freeze and spring snowmelt (Hall et al. 2009), so the ultimate residence time of stream primary producer C was likely driven by temperature and hydrologic scouring.

Respiration and incorporation into animal biomass are other probable fates for autochthonous C after short-term losses as DIC and DOC. Up to 29% of $^{13}C_{DIC}$ added to experimental flow channels was incorporated into protozoan grazers in a stream biofilm tracer study (Risse-Buhl et al. 2012). Lake $^{13}C_{DIC}$ tracer studies found up to 75% and 50% of newly fixed C in invertebrates (Solomon et al. 2008) and fish (Carpenter et al. 2005, Weidel et al. 2008), respectively. We did not separate detritus and associated heterotrophs from primary producer pools, but we assume heterotrophic microbes were labeled with newly fixed C given the tight coupling between autotrophs and associated heterotrophs. Grazing and movement of invertebrates and fishes may also have contributed to storage, downstream fluxes, and respiration of autotrophic C.

Fate of autochthonous C in streams

We suggest three distinct fates of newly fixed C in streams at two different time scales. One fate is fast turnover via respiration by primary producers and closely associated heterotrophs. The second is rapid exudation of DOC, which can fuel heterotrophic production and respiration. Time scales associated with these fates are hours to days. A small fraction of this released autochthonous DOC will travel downstream (we found 2% export relative to ^{13}C incorporation). The third fate is storage at a longer time scale of weeks or months; this C is that which likely supports a fraction of stream animal production. The rapid release of biologically available autochthonous DOC likely stimulates heterotrophic respiration (Tobias et al. 2007, Hotchkiss and Hall 2014), bacterial production (Cole et al. 1982, Farjalla et al. 2009), denitrification (Heffernan and Cohen 2010), and other biogeochemical processes that require OC. Increases in biologically available autochthonous OC could also prime the breakdown of more refractory OC (Farjalla et al. 2009, Hotchkiss et al. 2014, Kuehn et al. 2014) and may thus play a stronger role in C cycling than current regional and global budgets account for. We suspect autochthonous C stored in benthic OC is a primary food source for animals (Finlay et al. 2002) with longer-term storage and transport providing high quality OC to higher trophic levels. A large portion of autochthonous C remaining after short-term losses was exported from our study reach as suspended POC. When in transport, suspended POC might become more available for consumption by microbes and filter feeders. While biological processes are responsible for short-term exudation and respiration, physical processes likely drive the mobilization, consumption, and respiration of autochthonous C stored in the benthos.

Autochthonous C can play a substantial role in biogeochemical cycling and food webs in the time period between fixation and eventual loss as DIC. By using $^{13}C_{DIC}$ additions, we can trace and compare the fluxes and residence time of newly fixed C relative to major C fluxes in aquatic and terrestrial ecosystems. The rapid transfer of newly fixed C to DIC and DOC pools in French Creek is remarkably similar to fluxes measured in a range of ecosystems. Grassland and pasture $^{13}C_{DIC}$ tracer additions identified short-term (<2 d) peaks in exudation and respiration, 1–7 d turnover of new C in microbial biomass, and longer residence time (>1 wk) of remaining new C in soil (Butler et al. 2004, Leake et al. 2006, Kaštovská and Šantrůčková 2007). Peatland net $^{13}C_{DOC}$ exudation peaked 24 h after a $^{13}C_{DIC}$ pulse addition (Fenner et al. 2007). In subtidal marine benthos, 63% of newly fixed C was respired and 31% remained after 33 d (Oakes et al. 2012). We did not isolate turnover of newly fixed C in microbial biomass from bulk benthic OC pools, but subsequent whole-stream studies could use ^{13}C-phospholipid fatty acids and other stable isotope probing techniques to more specifically trace microbial pathways and turnover rates of newly fixed C. Moreover, future research that quantifies the fluxes and fate of older autochthonous C in addition to newly fixed C will greatly broaden our understanding of how C sources influence C fluxes and food webs over longer time scales.

The proportion of newly fixed C that is respired, exuded, or stored will likely change over time and among ecosystems. For example, freshwater and marine ^{13}C tracer studies found increases in new C exudation in the presence of higher nutrient concentrations (Van den Meersche et al. 2004, Lyon and Ziegler 2009), which may reduce the longer-term storage and availability of autochthonous C for animal consumers. We expect the residence time and fate of autochthonous and allochthonous C will differ in streams and rivers that vary in ecosystem size, productivity, connectivity with the landscape, and hydrological regime. Unlike C that accumulates in lake and marine sediments, in more

stable layers of terrestrial soil, and as wood in aquatic ecosystems, stream and river autochthonous C is less likely to be stored long-term (>1 y) unless deposited in a floodplain. The ultimate fate of autochthonous C exported downstream is unknown, but understanding this fate is needed for C budgets and likely varies with changes in stream and river hydrology, geomorphology, and rates of biological C consumption. Future research using $^{13}C_{DIC}$ tracers has the opportunity to better characterize freshwater ecosystems by linking the contributions of distinct C sources to whole-stream food web and C dynamics.

Acknowledgments

We thank P. Hellbaum, J. Neuwerth, C. Ruiz, and A. Saville for assistance in the field and laboratory. We also thank N. Swoboda-Colberg for setting up the GC to run SF_6 samples and P. Colberg for lab access. Comments from R. Sponseller, E. Pendall, M. Clementz, D. Willams, P. Colberg, and two anonymous reviewers greatly improved the manuscript. C. Cook and C. McDonald provided support at the University of Wyoming Stable Isotope Facility. We thank the University of Wyoming for coordinating and the U.S. Forest Service for approving our special use permit to conduct research in Medicine Bow National Forest. Funding for this project was provided by NSF DEB-1110831 awarded to E. R. Hotchkiss and R. O. Hall, Wyoming Experimental Program to Stimulate Competitive Research (EPSCoR), and a Dr. George E. Menkens Memorial Scholarship to E. R. Hotchkiss from the Zoology and Physiology Department, University of Wyoming.

Literature Cited

Aufdenkampe, A. K., E. Mayorga, P. A. Raymond, J. M. Melack, S. C. Doney, S. R. Alin, R. E. Aalto, and K. Yoo. 2011. Riverine coupling of biogeochemical cycles between land, oceans, and atmosphere. Frontiers in Ecology and the Environment 9:53–60.

Bade, D. L., S. R. Carpenter, J. J. Cole, M. L. Pace, E. Kritzberg, M. C. van de Bogert, R. M. Cory, and D. M. McKnight. 2007. Sources and fate of dissolved organic carbon in lakes as determined by whole-lake carbon isotope additions. Biogeochemistry 84:115–129.

Baines, S. B., and M. L. Pace. 1991. The production of dissolved organic matter by phytoplankton and its importance to bacteria: patterns across marine and freshwater systems. Limnology and Oceanography 36:1078–1090.

Battin, T. J., L. A. Kaplan, S. Findlay, C. S. Hopkinson, E. Marti, A. I. Packman, J. D. Newbold, and F. Sabater. 2008. Biophysical controls on organic carbon fluxes in fluvial networks. Nature Geoscience 1:95–100.

Bower, P. M., C. A. Kelly, E. J. Fee, J. A. Shearer, D. R. DeClercq, and D. W. Schindler. 1987. Simultaneous measurement of primary production by whole-lake and bottle radiocarbon additions. Limnology and Oceanography 32: 299–312.

Butler, J. L., P. J. Bottomley, S. M. Griffith, and D. D. Myrold. 2004. Contribution and turnover of recently fixed photosynthate in ryegrass rhizospheres. Soil Biology and Biochemistry 36:371–381.

Carpenter, S. R., J. J. Cole, M. L. Pace, M. Van de Bogert, D. L. Bade, D. Bastviken, C. M. Gille, J. R. Hodgson, J. F. Kitchell, and E. S. Kritzberg. 2005. Ecosystem subsidies: terrestrial support of aquatic food webs from ^{13}C addition to contrasting lakes. Ecology 86:2737–2750.

Cole, J. J., and N. F. Caraco. 2001. Carbon in catchments: connecting terrestrial carbon losses with aquatic metabolism. Marine and Freshwater Resources 52:101–110.

Cole, J. J., S. R. Carpenter, J. F. Kitchell, and M. L. Pace. 2002. Pathways of organic carbon utilization in small lakes: results from a whole-lake ^{13}C addition and coupled model. Limnology and Oceanography 47:1664–1675.

Cole, J. J., G. E. Likens, and D. L. Strayer. 1982. Photosynthetically produced dissolved organic carbon: an important carbon source for planktonic bacteria. Limnology and Oceanography 27:1080–1090.

Cole, J. J., et al. 2007. Plumbing the global carbon cycle: integrating inland waters into the terrestrial carbon budget. Ecosystems 10:171–184.

Farjalla, V. F., C. C. Marinho, B. M. Faria, A. M. Amado, F. de A. Esteves, R. L. Bozelli, and G. Giroldo. 2009. Synergy of fresh and accumulated organic matter to bacterial growth. Microbial Ecology 57:657–666.

Fenner, N., N. J. Ostle, N. McNamara, T. Sparks, H. Harmens, B. Reynolds, and C. Freeman. 2007. Elevated CO_2 effects on peatland community carbon dynamics and DOC production. Ecosystems 10:635–647.

Finlay, J. C., S. Khandwala, and M. E. Power. 2002. Spatial scales of carbon flow in a river food web. Ecology 83:1845–1859.

Fisher, S. G., and G. E. Likens. 1973. Energy flow in Bear Brook, New Hampshire: an integrative approach to stream ecosystem metabolism. Ecological Monographs 43:421–439.

Geyer, C. J., and L. T. Johnson. 2013. mcmc: Markov chain Monte Carlo. Package version 0.9-2. http://www.stat.umn.edu/geyer/mcmc/

Guillemette, F., S. L. McCallister, and P. A. del Giorgio. 2013. Differentiating the degradation dynamics of algal and terrestrial carbon within complex natural dissolved organic carbon in temperate lakes. Journal of Geophysical Research—Biogeosciences 118:1–11.

Hall, R. O. 1995. The use of a stable carbon isotope addition to trace bacterial carbon in a stream food web. Journal of the North American Benthological Society 14:269–277.

Hall, R. O., M. A. Baker, C. D. Arp, and B. J. Koch. 2009. Hydrologic control of nitrogen removal, storage, and export in a mountain stream. Limnology and Oceanography 54: 2126–2142.

Hall, R. O., and J. J. Beaulieu. 2013. Estimating autotrophic respiration in streams using daily metabolism data. Freshwater Science 32:507–516.

Hall, R. O., and J. L. Meyer. 1998. The trophic significance of bacteria in a detritus-based stream food web. Ecology 79: 1995–2012.

Heffernan, J. B., and M. J. Cohen. 2010. Direct and indirect coupling of primary production and diel nitrate dynamics in a subtropical spring-fed river. Limnology and Oceanography 55:677–688.

Hilborn, R., and M. Mangel. 1997. The ecological detective. Confronting models with data. Princeton University Press, Princeton, New Jersey, USA.

Hornberger, G. M., and M. G. Kelly. 1975. Estimation of atmospheric reaeration in a river using productivity analysis. Journal of the Environmental Engineering Division 101:729–739.

Hotchkiss, E. R., and R. O. Hall. 2010. Linking calcification by exotic snails to stream inorganic carbon cycling. Oecologia 163:235–245.

Hotchkiss, E. R., and R. O. Hall. 2014. High rates of daytime respiration in three streams: use of $\delta^{18}O_{O_2}$ and O_2 to model diel ecosystem metabolism. Limnology and Oceanography 39:798–810.

Hotchkiss, E. R., R. O. Hall, M. A. Baker, E. J. Rosi-Marshall, and J. L. Tank. 2014. Modeling priming effects on microbial consumption of dissolved organic carbon in rivers. Journal of Geophysical Research—Biogeosciences 119:982–995.

Johnson, L. T., et al. 2013. Quantifying the production of dissolved organic nitrogen in headwater streams using ^{15}N

tracer additions. Limnology and Oceanography 58:1271–1285.

Kaštovská, E., and H. Šantrůčková. 2007. Fate and dynamics of recently fixed C in pasture plant-soil system under field conditions. Plant Soil 300:61–69.

Kritzberg, E. S., J. J. Cole, M. L. Pace, and W. Graneli. 2005. Does autochthonous primary production drive variability in bacterial metabolism and growth efficiency in lakes dominated by terrestrial C inputs? Aquatic Microbial Ecology 38: 103–111.

Kuehn, K. A., S. N. Francoeur, R. H. Findlay, and R. K. Neely. 2014. Priming in the microbial landscape: periphytic algal stimulation of litter-associated microbial decomposers. Ecology 95:749–762.

Lang, S. Q., S. M. Bernasconi, and G. L. Früh-Green. 2011. Stable isotope analysis of organic carbon in small (μg C) samples and dissolved organic matter using a GasBench preparation device. Rapid Communications in Mass Spectrometry 26:9–16.

Lapierre, J.-F., F. Guillemette, M. Berggren, and P. A. del Giorgio. 2013. Increases in terrestrially derived carbon stimulate organic carbon processing and CO_2 emissions in boreal aquatic ecosystems. Nature Communications 4:2971.

Leake, J. R., N. J. Ostle, J. I. Rangel-Castro, and D. Johnson. 2006. Carbon fluxes from plants through soil organisms determined by field $^{13}CO_2$ pulse-labelling in an upland grassland. Applied Soil Ecology 33:152–175.

Lyon, D. R., and S. E. Ziegler. 2009. Carbon cycling within epilithic biofilm communities across a nutrient gradient of headwater streams. Limnology and Oceanography 54:439–449.

Marcarelli, A. M., C. V. Baxter, M. M. Mineau, and R. O. Hall. 2011. Quantity and quality: unifying food web and ecosystem perspectives on the role of resource subsidies in freshwaters. Ecology 92:1215–1225.

Middleburg, J. J., C. Barranguet, H. T. S. Boschkler, P. M. J. Herman, T. Moens, and C. H. R. Heip. 2000. The fate of intertidal microphytobenthos carbon: an in situ ^{13}C-labeling study. Limnology and Oceanography 45:1224–1234.

Minshall, G. W. 1978. Autotrophy in stream ecosystems. BioScience 28:767–771.

Minshall, G. W., K. W. Cummins, R. C. Petersen, C. E. Cushing, D. A. Bruns, J. R. Sedell, and R. L. Vannote. 1985. Developments in stream ecosystem theory. Canadian Journal of Fisheries and Aquatic Sciences 42:1045–1055.

Oakes, J. M., B. D. Eyre, and J. J. Middelburg. 2012. Transformation and fate of microphytobenthos carbon in a subtropical shallow subtidal sands: a ^{13}C-labeling study. Limnology and Oceanography 57:1846–1856.

Pace, M. L., J. J. Cole, S. R. Carpenter, J. F. Kitchell, J. R. Hodgson, M. C. Van der Bogert, D. L. Bade, E. S. Kritzberg, and D. Bastviken. 2004. Whole-lake carbon-13 additions reveal terrestrial support of aquatic food webs. Nature 427: 240–243.

Payn, R. A., M. N. Gooseff, B. L. McGlynn, K. E. Bencala, and S. M. Wondzell. 2009. Channel water balance and exchange with subsurface flow along a mountain headwater stream in Montana, United States. Water Resources Research 45:W11427.

R Development Core Team. 2012. R: a language and environment for statistical computing. R Foundation for Statistical Computing, Vienna, Austria. www.r-project.org

Raymond, P. A., et al. 2013. Global carbon dioxide emissions from inland waters. Nature 503:355–359.

Regnier, P., et al. 2013. Anthropogenic perturbation of the carbon fluxes from land to the ocean. Nature Geoscience 6: 597–607.

Risse-Buhl, U., N. Trefzger, A.-G. Seifert, W. Schönborn, G. Gleixner, and K. Küsel. 2012. Tracking the autochthonous carbon transfer in stream biofilm food webs. FEMS Microbiology Ecology 79:118–131.

Roberts, B. J., P. J. Mulholland, and W. R. Hill. 2007. Multiple scales of temporal variability in ecosystem metabolism rates: results from 2 years of continuous monitoring in a forested headwater stream. Ecosystems 10:588–606.

Solomon, C., S. Carpenter, J. Cole, and M. Pace. 2008. Support of benthic invertebrates by detrital resources and current autochthonous primary production: results from a whole-lake ^{13}C addition. Freshwater Biology 53:42–54.

Thorp, J. H., and M. D. Delong. 2002. Dominance of autochthonous autotrophic carbon in food webs of heterotrophic rivers. Oikos 96:543–550.

Tobias, C. R., J. K. Böhlke, and J. W. Harvey. 2007. The oxygen-18 isotope approach for measuring aquatic metabolism in high-productivity waters. Limnology and Oceanography 52:1439–1453.

Van den Meersche, K., J. J. Middelburg, K. Soetaert, P. Van Rijswijk, H. T. S. Boschker, and C. H. R. Heip. 2004. Carbon-nitrogen coupling and algal-bacterial interactions during and experimental bloom: modeling a ^{13}C tracer experiment. Limnology and Oceanography 49:862–878.

Wallace, J. B., S. L. Eggert, J. L. Meyer, and J. R. Webster. 1997. Multiple trophic levels of a forest stream linked to terrestrial litter inputs. Science 277:102–104.

Wanninkhof, R. 1992. Relationship between gas exchange and wind speed over the ocean. Journal of Geophysical Research 97:7373–7382.

Webster, J. R. 2007. Spiraling down the river continuum: stream ecology and the U-shaped curve. Journal of the North American Benthological Society 26:375–389.

Webster, J. R., E. F. Benfield, T. P. Ehrman, M. A. Schaeffer, J. L. Tank, J. J. Hutchens, and D. J. D'Angelo. 1999. What happens to allochthonous material that falls into streams? A synthesis of new and published information from Coweeta. Freshwater Biology 41:687–705.

Weidel, B., S. Carpenter, J. Cole, J. Hodgson, J. Kitchell, M. Pace, and C. Solomon. 2008. Carbon sources supporting fish growth in a north temperate lake. Aquatic Sciences 70:446–458.

Wollheim, W. M., B. J. Peterson, L. A. Deegan, J. E. Hobbie, B. Hooker, W. B. Bowden, K. J. Edwardson, D. B. Arscott, A. E. Hershey, and J. Finlay. 2001. Influence of stream size on ammonium and suspended particulate nitrogen processing. Limnology and Oceanography 46:1–13.

Supplemental Material

Ecological Archives

Appendices A–C are available online: http://dx.doi.org/10.1890/14-0631.1.sm